[redacted]

NACA

RESEARCH MEMORANDUM

EFFECTS OF ROCKET-ARMAMENT EXHAUST GAS ON THE PERFORMANCE OF A SUPERSONIC-INLET J34-TURBOJET-ENGINE INSTALLATION AT MACH 2.0

By Milton A. Beheim and Philip J. Evans

Lewis Flight Propulsion Laboratory
Cleveland, Ohio

[redacted]

NATIONAL ADVISORY COMMITTEE
FOR AERONAUTICS

WASHINGTON
February 20, 1956

[redacted]

[redacted]

Classification cancelled (or changed to Unclassified)

By Authr NASA Tech Pub Announcement #29
(OFFICER AUTHORIZED TO CHANGE)

By ..... 27 Sept 66

..... NF .....
(GRADE OF OFFICER MAKING CHANGE)

27 Sept 66
DATE

NATIONAL ADVISORY COMMITTEE FOR AERONAUTICS

RESEARCH MEMORANDUM

EFFECTS OF ROCKET-ARMAMENT EXHAUST GAS ON THE PERFORMANCE OF A SUPERSONIC-INLET J34-TURBOJET-ENGINE INSTALLATION AT MACH 2.0

By Milton A. Beheim and Philip J. Evans

SUMMARY

An investigation of the effects of rocket-armament-exhaust-gas ingestion on the performance of a supersonic-inlet J34-turbojet-engine installation was conducted at Mach 2.0. The increase in compressor-inlet temperature resulted in decreased corrected engine air flow and caused the inlet to operate at decreased mass-flow ratios. The inlet normal shock fluctuated rapidly during this disturbance, particularly when the inlet was forced to enter a region where buzz ordinarily occurred. Temperatures increased throughout the engine, and pressures generally decreased. Engine speed increased when the inlet temperature rise was large, but corrected engine speed decreased. Compressor pressure ratio remained essentially constant.

INTRODUCTION

Flight experience has shown that the firing of rocket armament from turbojet aircraft can affect engine operation if the rocket exhaust enters the inlet. An analysis of this problem (ref. 1) showed that the hot rocket gases tend to produce a sudden reduction in corrected engine speed and air flow. The final effect is a reduction in both the compressor stall margin and the combustor flame-out margin. Also, for supersonic aircraft an additional factor, the air inlet, must be considered; the decrease in air flow may force subcritical inlet operation, and in some cases buzz might result. The disturbance also may influence the inlet and engine controls.

As a preliminary evaluation of the magnitude of such disturbances, armament rockets were fired ahead of a J34-turbojet-inlet combination at a free-stream Mach number of 2.0 in the Lewis 8- by 6-foot wind tunnel. The results of this study are reported herein. (The performances of the inlet and the engine without the rockets are reported in refs. 2 and 3, respectively.)

[redacted]

[redacted]

APPARATUS AND PROCEDURE

A schematic diagram of the nacelle installation is presented in figure 1(a). Although the J34 engine was not designed for supersonic flight, it was used in this test because it was readily available and small enough not to cause tunnel blockage. A fixed-geometry convergent nozzle was used on the engine, and engine fuel flow was manually controlled. The inlet employed a 25°-half-angle cone, which could be translated from an angle θ_l of 53.6° to 38.4° without internal contraction at any position. (Symbols are defined in appendix A.) The bypass shown in figure 1 was not used for these tests. A screen was installed ahead of the compressor to provide some protection from debris from the rockets.

From a station about 41 feet upstream of the model in the subsonic part of the tunnel, 2.75-inch air-to-air folding-fin rockets were fired (fig. 1(b)). Burning time was about 1.8 seconds, combustion-chamber pressure was about 1100 psi, and exhaust-gas total temperature was about 4500° R. For further specifications see reference 4. The orientation of the four rockets with respect to the cowl lip is shown in figure 1(c). The distance between rocket centers was equal to the cowl-lip radius. Rocket position will be referred to by the number indicated in the figure. Because of the widely varying free-stream conditions from the rocket firing station to the inlet, rocket position has significance only in that it was a means of varying the amount of rocket exhaust that entered the inlet. For these tests the metal caps in the rocket exhaust nozzles were removed, and the electric firing wire was as short as possible.

Transient total pressures and temperatures at the compressor inlet and exit and in the engine tail pipe were detected with fast-acting pickups and recorded on oscillographs. Two high-response-rate thermocouples were installed at the compressor inlet on opposite sides of the duct, but at all other stations measurements were made with single pickups. High-speed schlieren motion pictures were taken of the inlet during the disturbance.

The simulated pressure altitude in the tunnel test section was about 35,000 feet. The tunnel static temperature, however, was about -140° F.

RESULTS AND DISCUSSION

Rockets were fired for two different spike positions and with the engine either at high or low speed. The diffuser performance without the rockets for these spike positions is shown in figure 2. For

$\theta_l = 51^\circ$ the oblique shock was situated well within the cowling during supercritical operation, and the inlet did not buzz over the air-flow range investigated. For the other spike position, $\theta_l = 42^\circ$, the oblique shock was situated slightly ahead of the cowl lip during supercritical operation. In this case the inlet buzzed at mass-flow ratios less than 0.92 but became stable again at mass-flow ratios less than 0.65. Arrows on the figure indicate the steady-state operating condition just before rocket firing. It can be seen that when firing with $\theta_l = 51^\circ$ the inlet was operating subcritically, and initial corrected engine speed was either about 8200 or 9000 rpm. For $\theta_l = 42^\circ$ the inlet was slightly supercritical at the time of firing, and the corrected engine speed was about 11,200 rpm.

3846

Instantaneous temperatures and pressures through the engine during the rocket burning with $\theta_l = 51^\circ$ and the engine at low speed are presented in figures 3(a) to (c). These copies show accurately only significant variations, and no attempt has been made to exactly duplicate the small, erratic fluctuations recorded on the original traces. Figure 3(a) shows the disturbances resulting when a single rocket was fired from location 1 with a corrected engine speed of 8200 rpm. Data of figures 3(b) and (c) were taken when a rocket was fired from locations 2 and 3, respectively, with a corrected engine speed of about 9000 rpm. As expected, the disturbances were greater with rockets more nearly alined with the inlet.

CE-1 back

Burning time of the rockets was about 1.8 seconds and the disturbances in the engine lasted less than about 3 seconds in all cases. As expected, temperatures increased throughout the engine; however, the increase in tail-pipe temperature was small. Total pressures generally decreased, particularly during the short time interval when the compressor-inlet temperature was highest. The compressor-inlet pressure trace (and also the motion pictures) indicated rapid fluctuations of the normal shock.

Pressure and temperature histories during rocket burning with the engine at a higher initial corrected speed (about 11,200 rpm) and with $\theta_l = 42^\circ$ are shown in figures 3(d) to (f). Firing single rockets from locations 2 and 3 gave the data of figures 3(d) and (e), respectively. The trends in temperatures and pressures were about the same as with the engine at low speed; but the magnitude of the disturbances, particularly in pressures, was greater. The fluctuations of the diffuser normal shock were also greater, probably because inlet operation was initially near a buzz region and, as a result of the temperature increase, would enter the buzz region.

Data for simultaneous firing of the three rockets positioned at locations 2, 3, and 4 are presented in figure 3(f). The disturbances

throughout the engine were much greater than those resulting from single rocket firings. With a maximum average increase in compressor-inlet temperature of 360° F, compressor-exit and tail-pipe temperatures increased as much as 150° and 200° F, respectively. Simultaneously, the compressor-exit pressure decreased 19 percent, and tail-pipe pressure decreased 24 percent.

A trace is shown in figure 3(f) of the transient engine speed. During this rocket firing the engine speed increased as much as 1070 rpm within 1.4 seconds and momentarily was 450 rpm over the rated speed of 12,500 rpm, but corrected engine speed decreased. For all other firings the engine-speed trace was not considered reliable. However, the change in engine speed as observed on the tachometer was small.

Flame-out did not occur during any firing and was not expected because of the fairly high pressure level of the tunnel. As stated earlier, rocket location in itself had no significance, but was only a means to vary the amount of rocket exhaust gas that entered the inlet. The concentration of rocket exhaust gas in the engine air flow was estimated from the average inlet temperature rise as indicated in appendix B. The maximum concentration for each of the different firings is shown in figure 4. The maximum concentration varied between 1 and 5 percent of the engine air flow before rocket firing.

From a time integration of the rocket-exhaust-gas concentration (appendix B), the fraction of total rocket propellant that entered the engine was also estimated. These results are presented in figure 5 for each of the rocket firings. Between about 5 and 20 percent of the total propellant entered the engine.

Because of the sudden increase in compressor-inlet temperature, corrected engine speed and air flow decreased. This decrease in corrected air flow through the inlet resulted in subcritical spillage with $\theta_l = 42°$ and increased subcritical spillage with $\theta_l = 51°$. In figure 6 the variation of inlet mass-flow ratio with normal-shock-position ratio (as determined from schlieren photos without the presence of the rockets) is shown for each of the spike positions. The operating conditions of the inlet just before rocket firings with corrected engine speeds of 9000 and 11,200 rpm are indicated by arrows. The approximate maximum extent of the normal-shock disturbance during the rocket burning as determined from high-speed schlieren motion pictures is also indicated.

With $\theta_l = 51°$ the movement of the shock was about the same when a rocket was fired from either location 2 or 3. When it was fired from location 1, the disturbance (not shown) was slightly less than that shown for the other locations. In general, the shock moved upstream from its initial subcritical position as the rocket began to burn, but

toward the end of the disturbance moved back slightly to a location downstream of its initial position. Although the inlet did not buzz over the air-flow range investigated without the rockets with $\theta_l = 51^\circ$, the normal shock fluctuated locally very rapidly during the rocket burning.

At $\theta_l = 42^\circ$ during the rocket burning the normal shock entered from its initially supercritical position a region where without the rockets buzz had occurred. The normal shock again fluctuated very rapidly, but with this spike position the movement of the normal shock during a fluctuation was greater. After moving out on the spike the shock would move back entirely into the inlet in a manner often characteristic of buzz. The minimum corrected engine speed during the multirocket firing was determined (from the engine-speed trace and average compressor-inlet temperature rise) to be about 9650 rpm. From engine and inlet performance without the rockets, the corresponding minimum inlet mass-flow ratio without considering effects of buzz was estimated and is indicated on the figure. The shock movement, however, was appreciably greater than expected from this estimate and thus indicated that inlet buzz probably occurred as it did during operation without the rockets.

The estimated variation of compressor pressure ratio with corrected engine speed during the miltirocket firing is presented in figure 7. The time after the disturbance reached the compressor inlet is indicated at several points on the curve. Because the amplitude of the compressor-inlet pressure pulsations became particularly large after $t = 0.85$ second, the accuracy of a computed compressor pressure ratio is in doubt for $t > 0.85$ second and that part of the curve is indicated by a dashed line. During burning the pressure ratio varied by less than ± 10 percent from the initial value, while corrected speed decreased by about 1600 rpm. For reference an equilibrium engine operating line, determined when the rockets were not present, and also the approximate variation in Reynolds number index (defined as $\delta_3/\varphi_3\sqrt{\theta_3}$) during rocket burning are indicated on the figure. Although the compressor was operating for about a second during the rocket burning in a region where with steady-state operation compressor stall might have occurred and compressor-exit pressure decreased and fluctuated as shown in earlier figures, there were no positive indications of stall.

Debris resulting from the multirocket burning entered the inlet and caused some damage. A photograph of the protective screen installed ahead of the compressor is shown in figure 8. A large hole was torn in the screen at the bottom, and some of the compressor blades were nicked. This damage may have resulted from impact with pieces of unburnt propellant, the firing wire, or perhaps pieces of the plastic liner in the rocket. Several pieces of this plastic can be seen on the screen in

the photograph. There is also an indentation in the upper left-hand corner of the screen caused by a piece of plastic. As stated earlier, the metal caps in the rocket nozzle were removed beforehand. Presumably these metal caps and the firing wire would remain in the launcher in an airplane installation and would not cause difficulty.

SUMMARY OF RESULTS

In an investigation of the effects of rocket-armament exhaust gas on the performance of a supersonic-inlet J34-turbojet-engine installation at Mach 2.0, the following results were obtained:

1. The decrease in corrected engine air flow resulting from the increased compressor-inlet temperature during rocket burning caused the inlet to operate more subcritically. The inlet normal shock fluctuated rapidly during this disturbance, particularly when the inlet was forced to enter a region where during normal engine operation buzz had occurred.

2. With a maximum average increase in compressor-inlet temperature of 360° F (the highest investigated) and with a corrected engine speed of 11,200 rpm, compressor-exit and tail-pipe temperatures increased as much as 150° and 200° F, respectively. Simultaneously compressor-exit pressure decreased 19 percent, and tail-pipe pressure decreased 24 percent. Engine speed increased 1070 rpm within 1.4 seconds and momentarily was 450 rpm over rated speed. Although corrected engine speed decreased as much as about 1600 rpm, compressor pressure ratio did not vary by more than ±10 percent.

3. Flame-out did not occur, nor were there any positive indications of compressor stall.

4. Debris resulting from the rocket burning entered the inlet and damaged a compressor protective screening and slightly dented some compressor blades.

Lewis Flight Propulsion Laboratory
National Advisory Committee for Aeronautics
Cleveland, Ohio, November 29, 1955

APPENDIX A

SYMBOLS

The following symbols are used in this report:

A	compressor rotor frontal area
c_p	specific heat at constant pressure
h	enthalpy
L	horizontal distance from cone tip to cowl lip
l	horizontal distance from normal shock to cowl lip during subcritical operation
m	mass flow
N	engine rotational speed, rpm
P	total pressure
T	total temperature
t	time after disturbance reaches compressor face, sec
W	weight
w	weight-flow rate
δ	ratio of total pressure to NACA standard sea-level pressure, P/2116
θ	ratio of total temperature to NACA standard sea-level temperature, T/519
θ_l	cowl-lip-position parameter defined as angle between axis of spike and line joining cone apex and cowl lip
θ_s	conical shock angle
φ	ratio of kinematic viscosity to NACA standard sea-level kinematic viscosity

[redacted]

Subscripts:

a	air
g	rocket exhaust gas
0	conditions in free-stream maximum-capture area of inlet
3	compressor face
4	compressor exit
5	tail pipe

APPENDIX B

ESTIMATES OF AMOUNT OF ROCKET EXHAUST GAS ENTERING INLET

The instantaneous concentration of rocket exhaust gas in the engine was estimated by equating total enthalpies at the compressor inlet as follows:

$$hw_3 = h_a(w_3 - w_{g,3}) + h_g w_{g,3}$$

Solving for the concentration gives

$$\frac{w_{g,3}}{w_3} = \frac{h - h_a}{h_g - h_a}$$

Assuming $c_{p,3} = c_{p,a,3}$ then

$$\frac{w_{g,3}}{w_3} = \frac{c_{p,a}\Delta T_3}{c_{p,g}T_g - c_{p,a}T_a}$$

With the assumptions $c_{p,a} = 0.24$, $c_{p,g} = 0.443$, and $T_g = 4500^\circ$ R, the equation becomes

$$\frac{w_{g,3}}{w_3} = \frac{\Delta T_3}{8310 - T_a}$$

(This concentration may be slightly low because the assumption of a constant $c_{p,g}$ overestimates h_g somewhat.)

The fraction of the total weight of propellant that entered the engine was estimated as follows:

$$\frac{W_g}{W_{propellant}} = \frac{w_{a,3_{steady\ state}}}{W_{propellant}} \int_0^t \frac{w_{g,3}}{w_3}\, dt$$

(The assumption that the weight flow of air through the engine was constant throughout the disturbance perhaps overestimates the fraction since the air-flow rate actually decreased an unknown amount.)

REFERENCES

1. Childs, J. Howard, Kochendorfer, Fred D., Lubick, Robert J., and Friedman, Robert: Stall and Flame-Out Resulting from Firing of Armament. NACA RM E55E25, 1955.

2. Beheim, Milton A., and Englert, Gerald W.: Effects of a J34 Turbojet Engine on Supersonic Diffuser Performance. NACA RM E55I21, 1955.

3. Beke, A., Englert, G. W., and Beheim, M. A.: Effect of an Adjustable Supersonic Inlet on the Performance up to Mach Number of 2.0 of a J34 Turbojet Engine. NACA RM E55I27, 1955.

4. Staff, Rockets and Explosives Department: 2.75-Inch Air-to-Air Folding-Fin Rocket (AAFFR). Description and Instructions for Use. NAVORD Rep. 1263, U.S. Naval Ord. Test Station, Oct. 6, 1950.

[redacted]

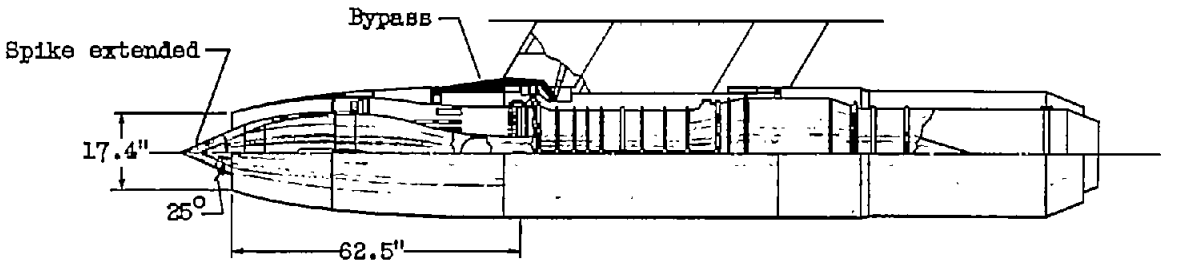

(a) Nacelle installation of J34 turbojet engine.

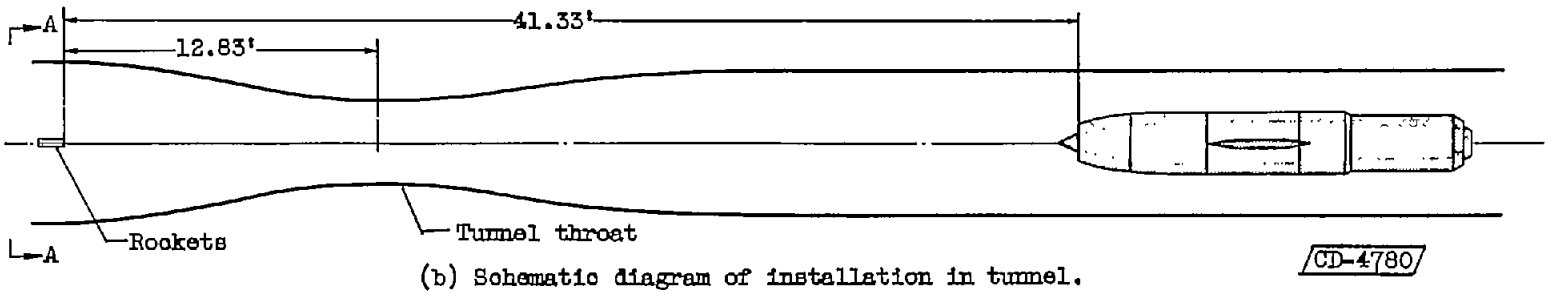

(b) Schematic diagram of installation in tunnel.

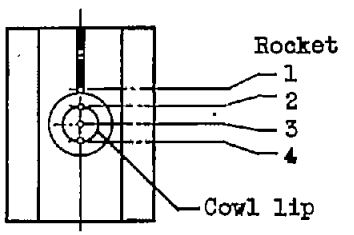

(c) Section A-A. Rocket location relative to cowl lip.

Figure 1. - Test apparatus.

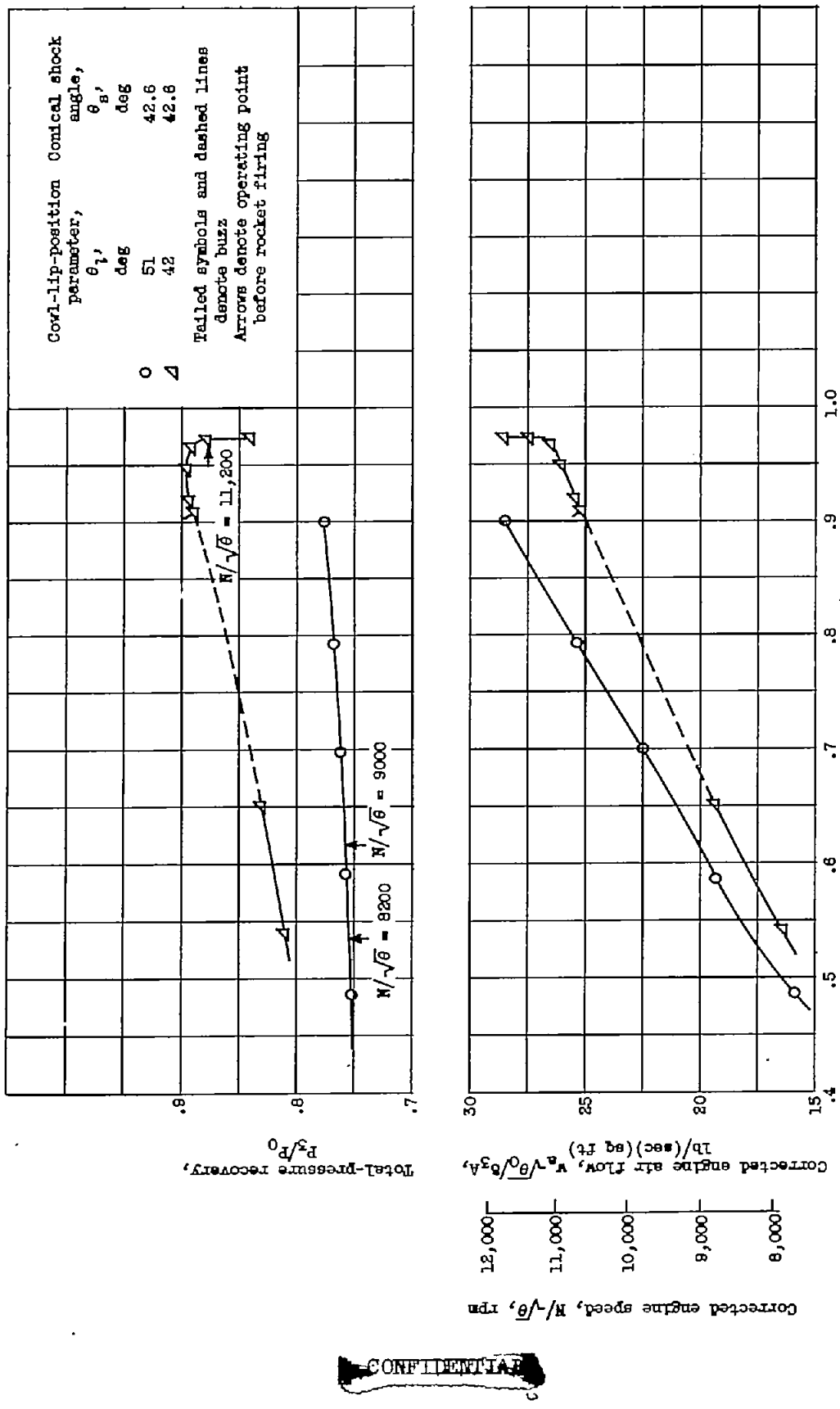

Figure 2. - Diffuser performance (data from ref. 2).

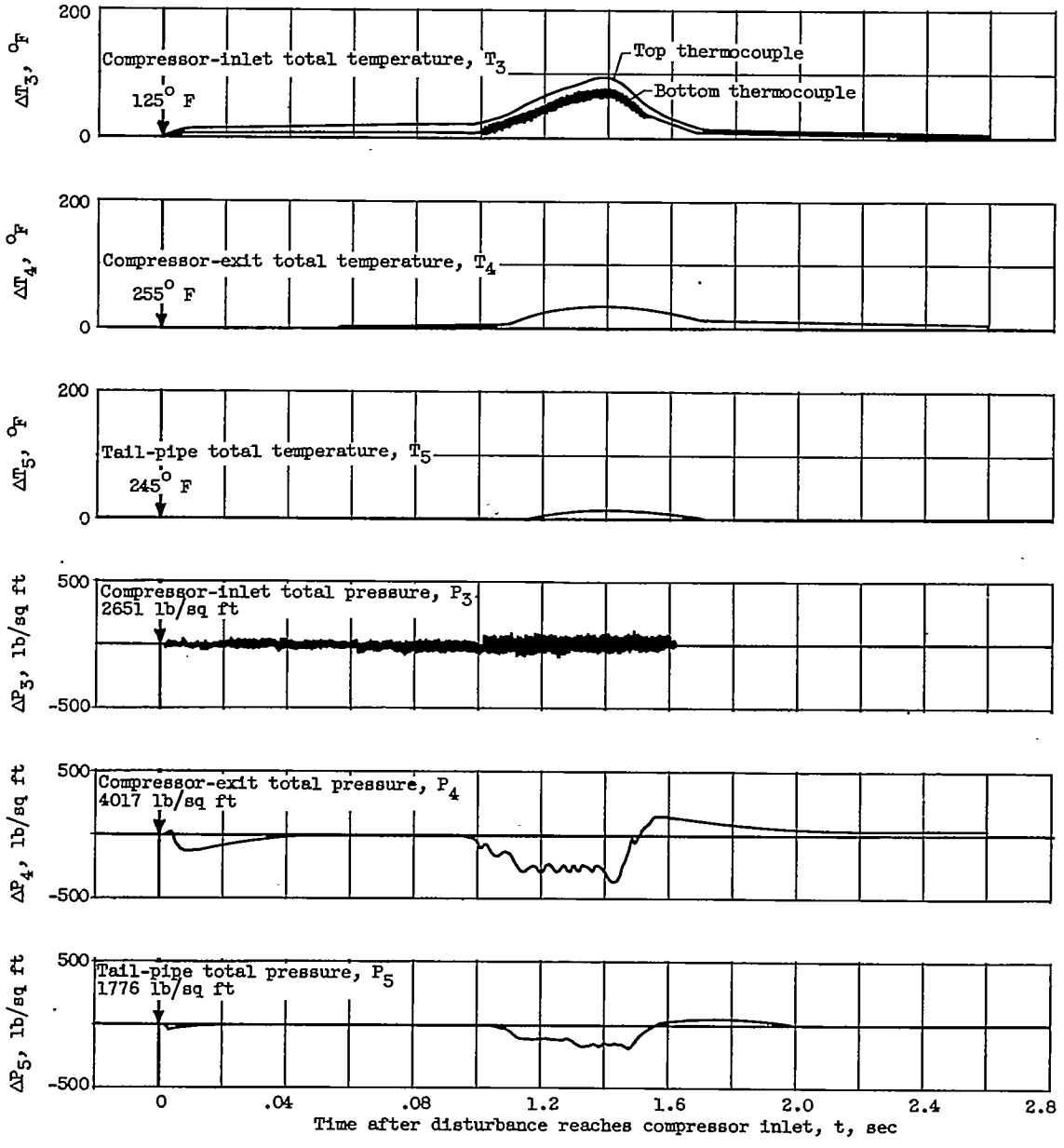

(a) Rocket 1. Initial corrected engine speed, 8200 rpm; cowl-lip-position parameter, 51°.

Figure 3. - Temperature and pressure disturbances through nacelle during rocket burning.

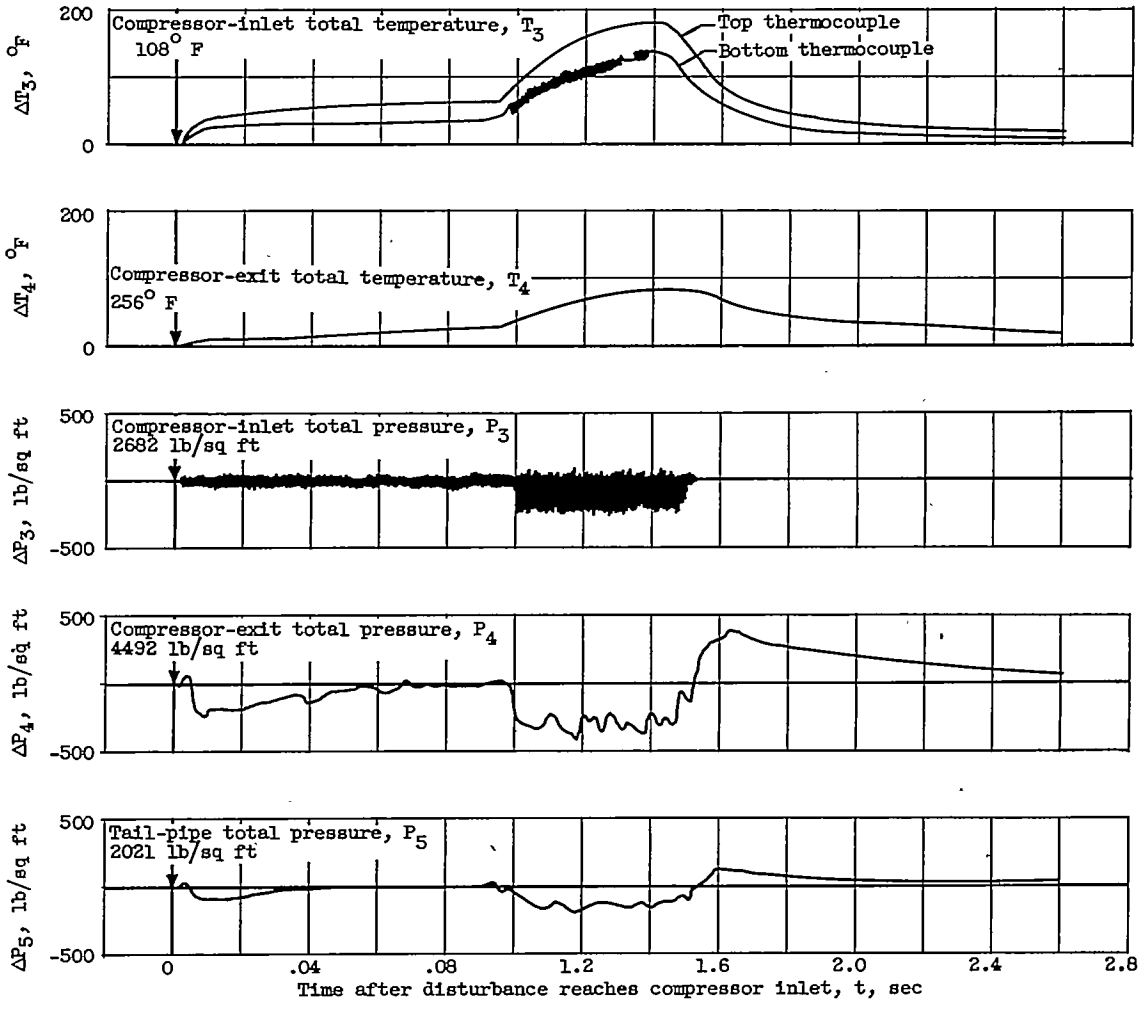

(b) Rocket 2. Initial corrected engine speed, 9000 rpm; cowl-lip-position parameter, 51°.

Figure 3. - Continued. Temperature and pressure disturbances through nacelle during rocket burning.

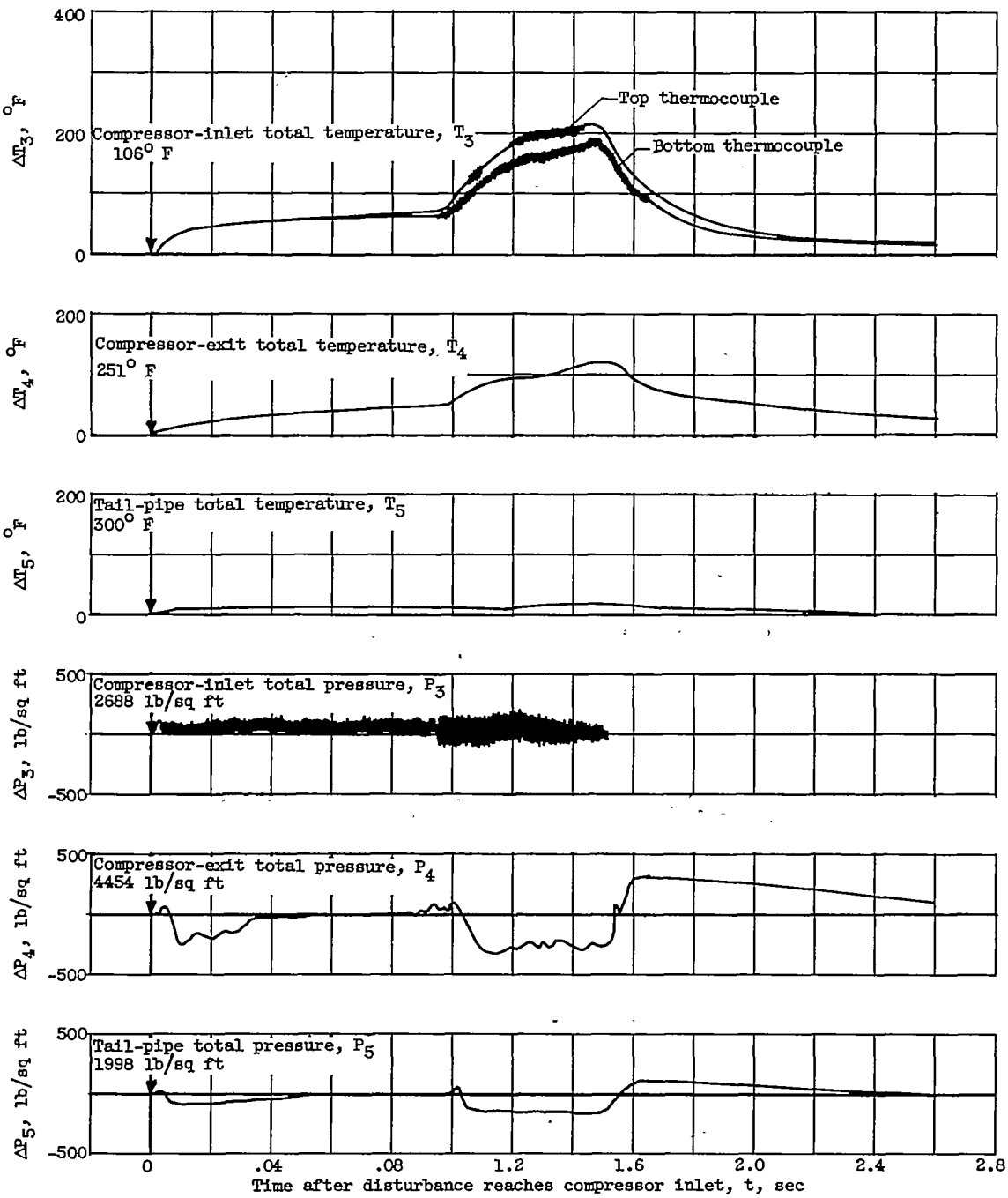

(c) Rocket 3. Initial corrected engine speed, 9000 rpm; cowl-lip-position parameter, 51°.

Figure 3. - Continued. Temperature and pressure distribution through nacelle during rocket burning.

[redacted]

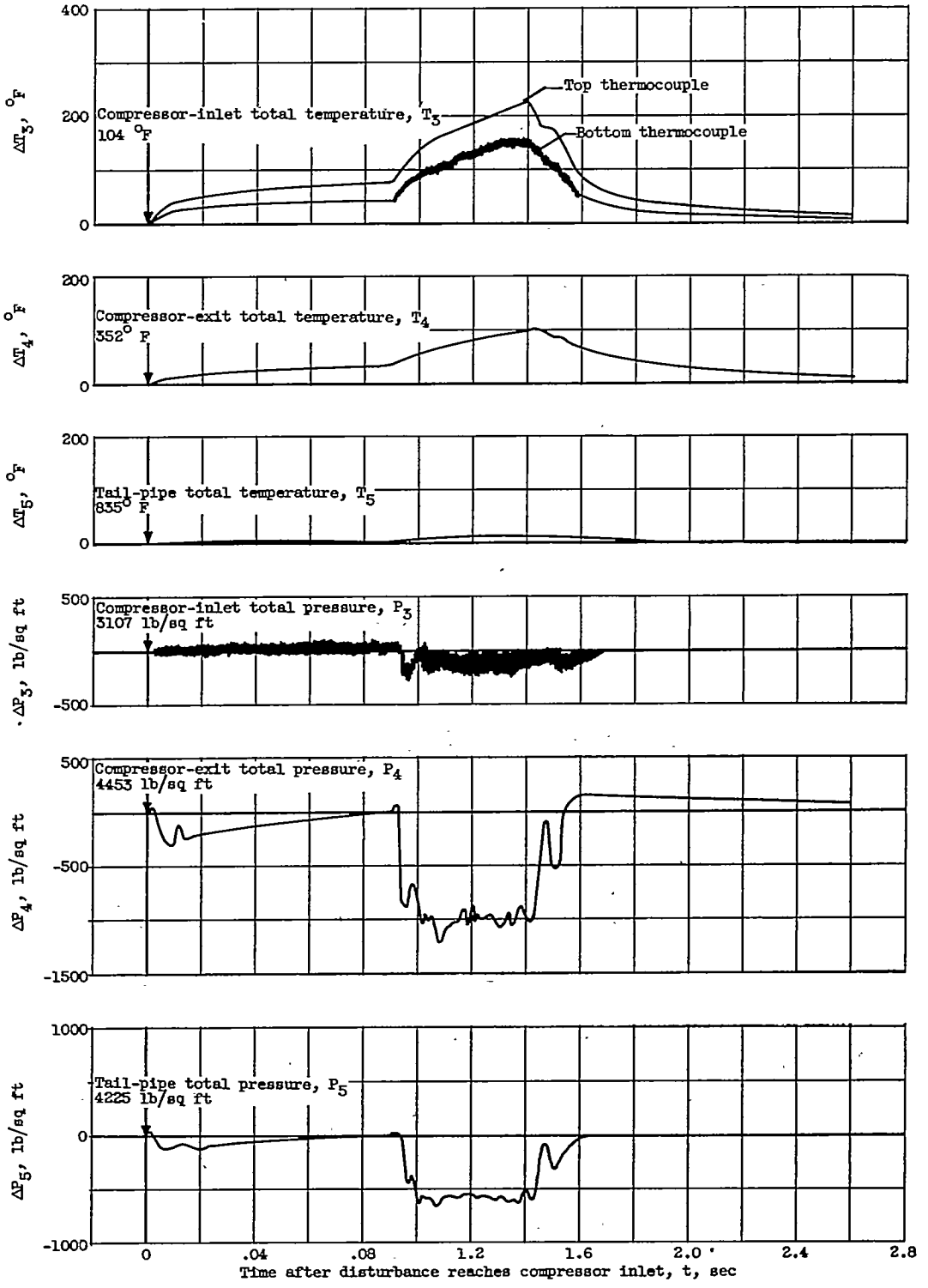

(d) Rocket 2. Initial corrected engine speed, 11,200 rpm; cowl-lip-position parameter, 42°.

Figure 3. - Continued. Temperature and pressure distribution through nacelle during rocket burning.

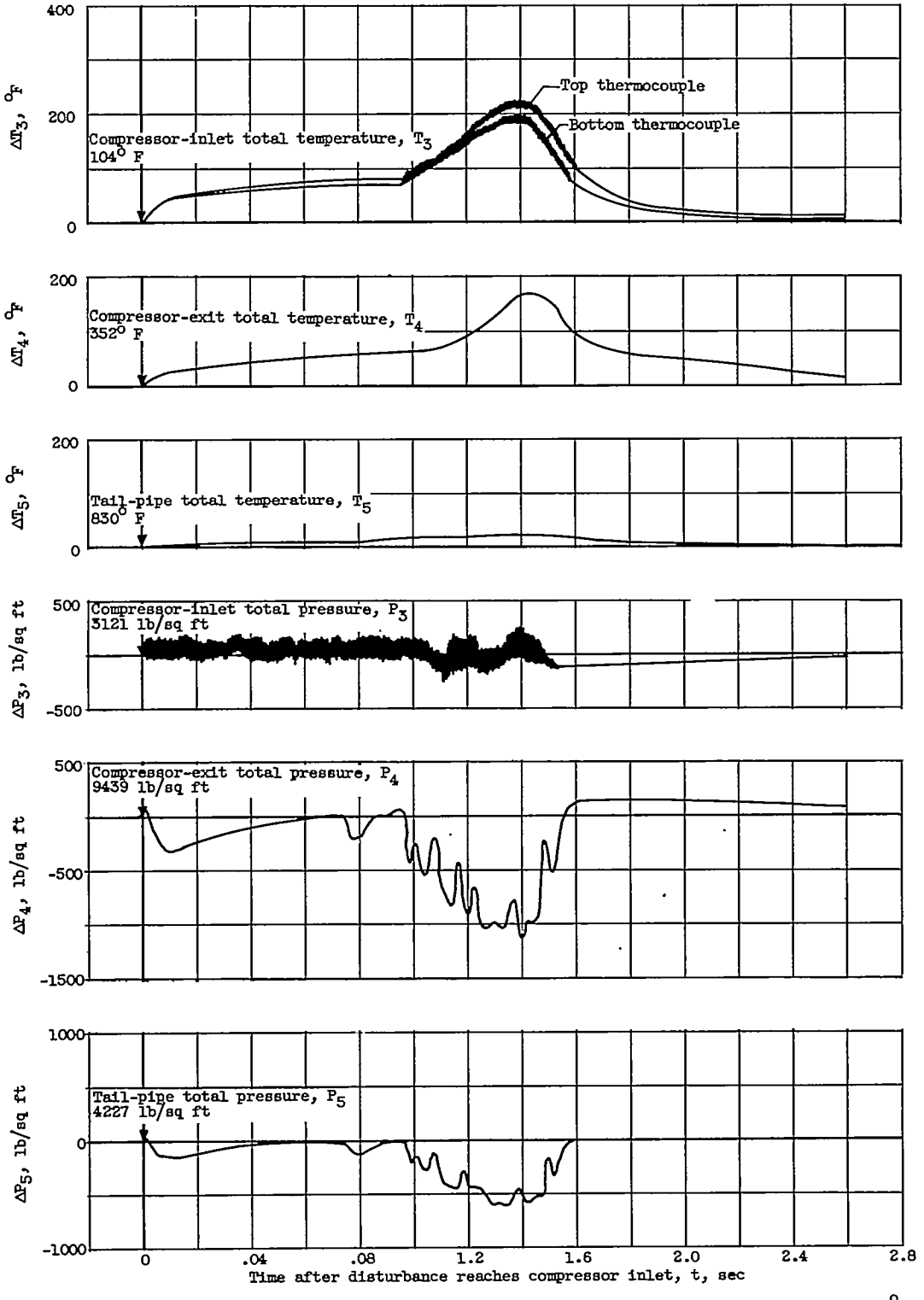

(e) Rocket 3. Initial corrected engine speed, 11,200 rpm; cowl-lip-position parameter, 42°.

Figure 3. - Continued. Temperature and pressure distribution through nacelle during rocket burning.

[redacted]

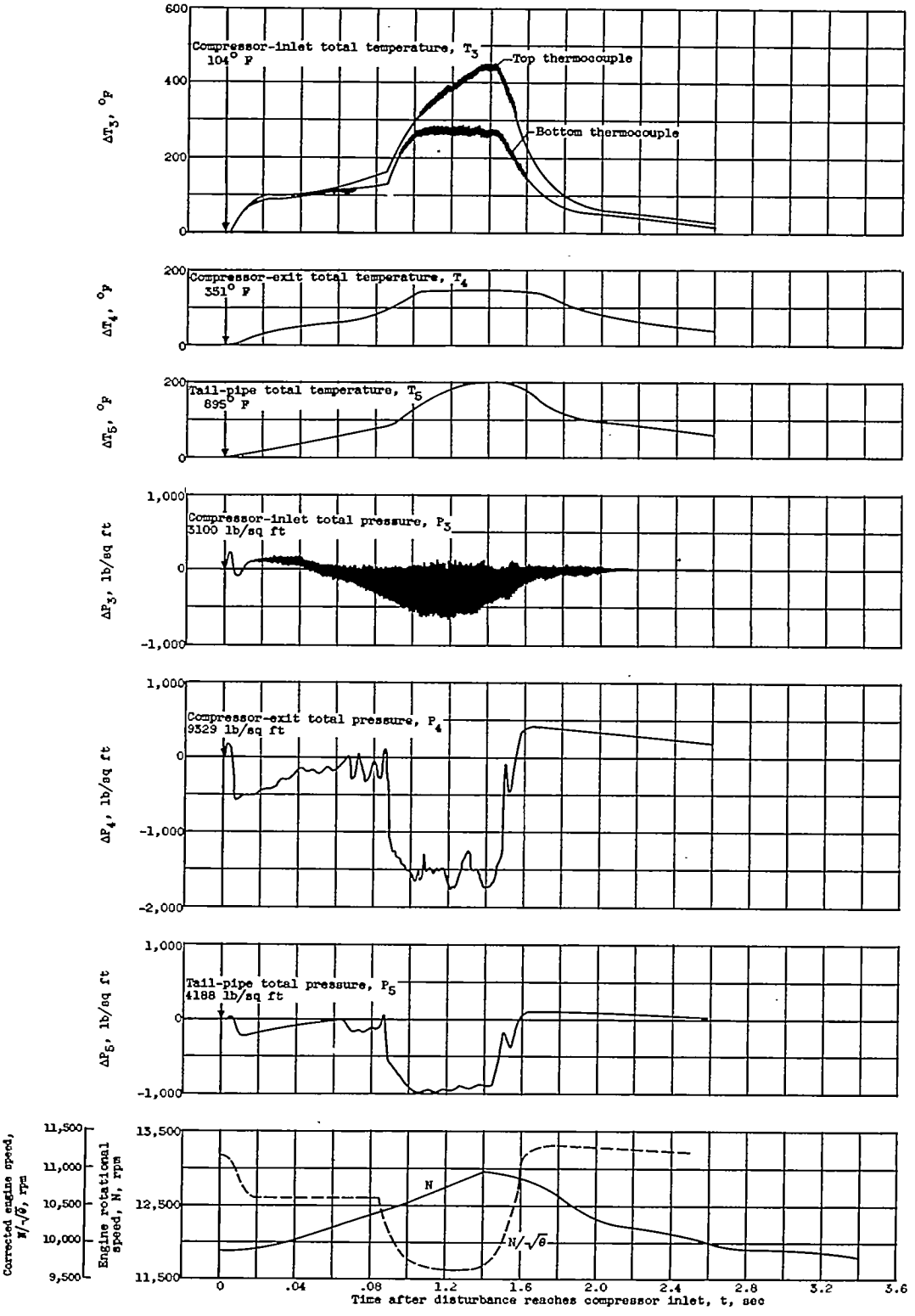

(f) Rockets 2, 3, and 4. Initial corrected engine speed, 11,200 rpm; cowl-lip-position parameter, 42°.

Figure 3. - Concluded. Temperature and pressure distribution through nacelle during rocket burning.

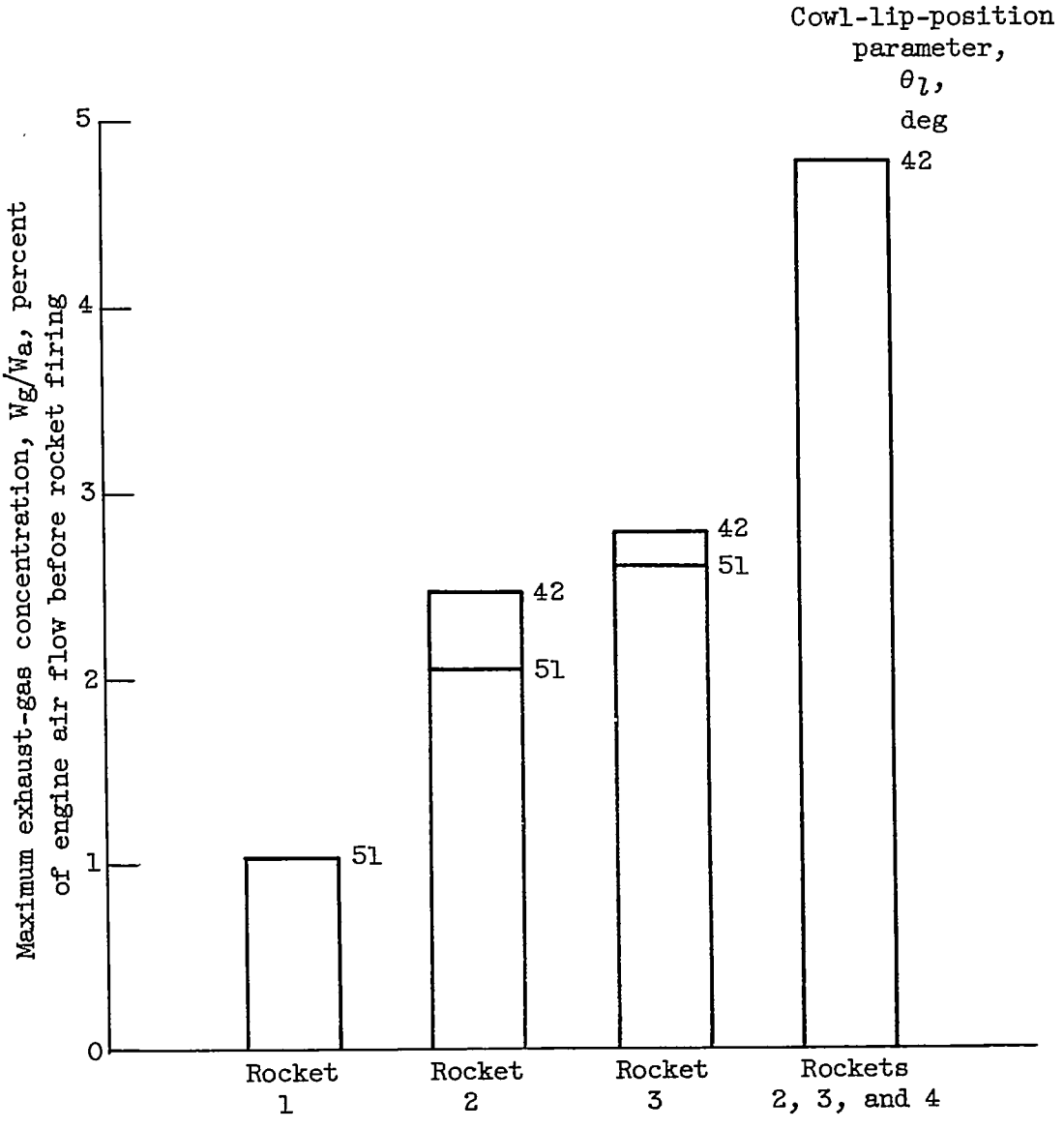

Figure 4. - Maximum rocket-exhaust-gas concentration in engine.

[redacted]

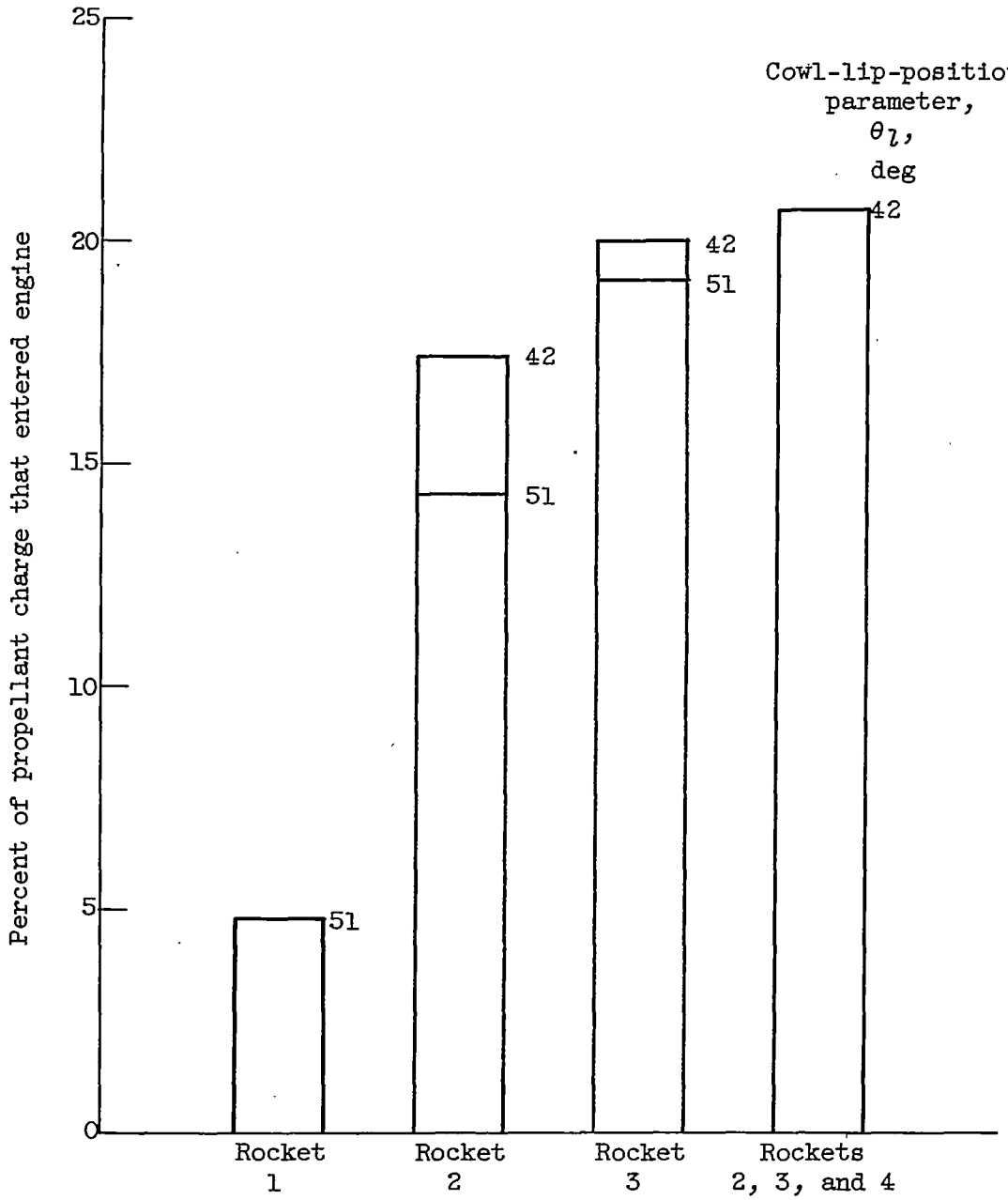

Figure 5. - Percent of propellant charge that entered engine.

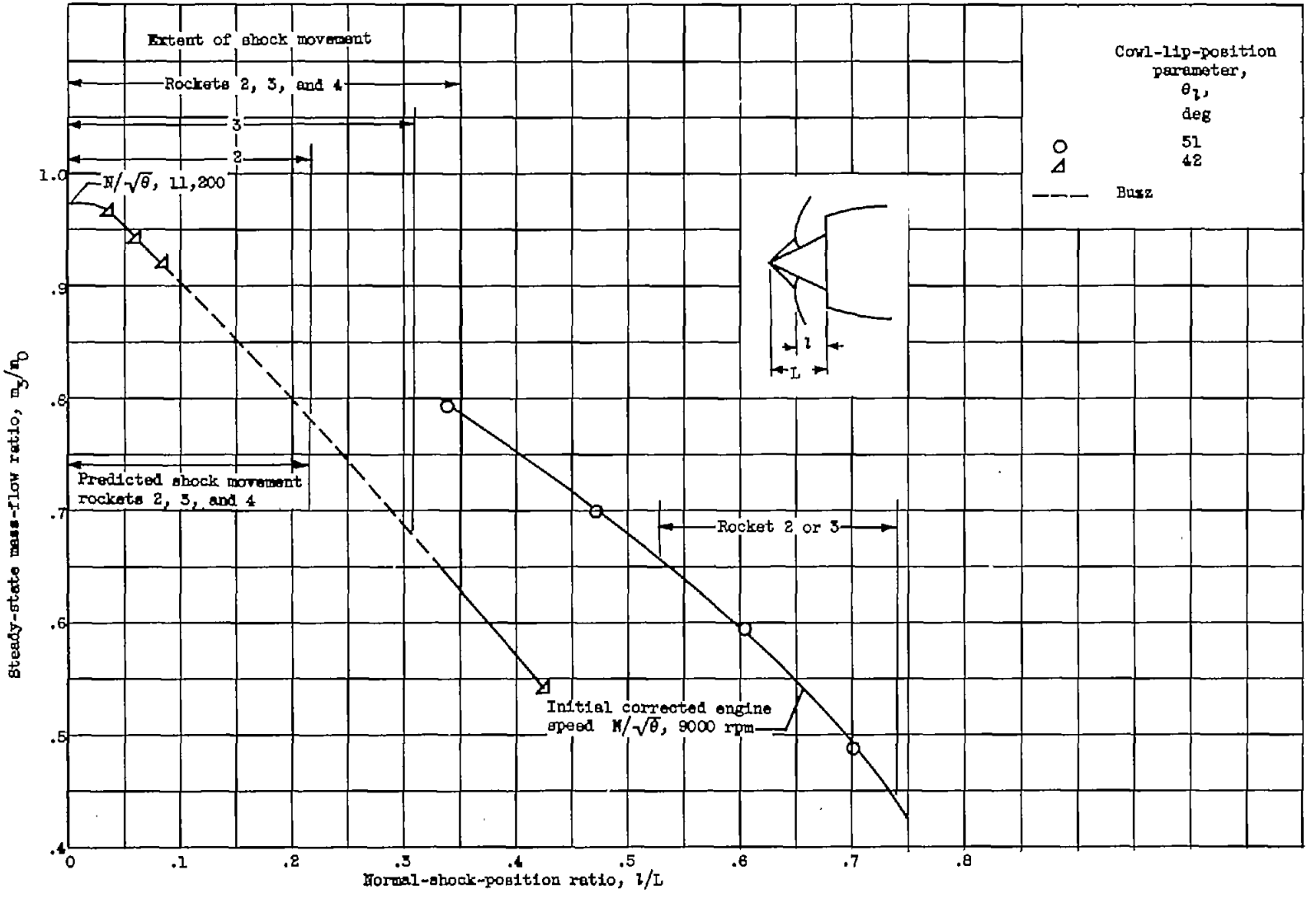

Figure 6. - Maximum extent of disturbance of normal shock during rocket burning.

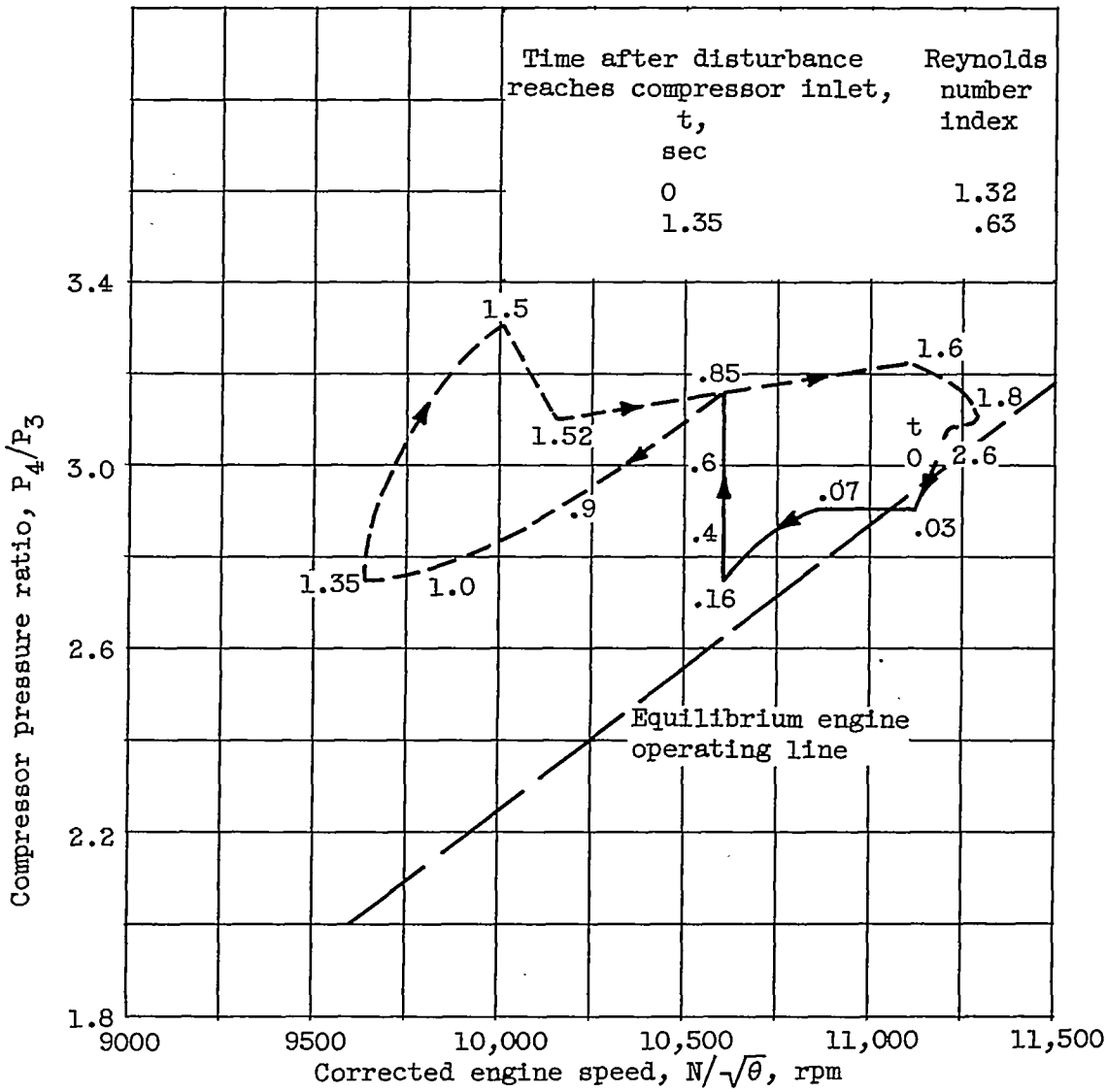

Figure 7. - Variation of compressor pressure ratio with corrected speed during rocket burning. Rockets 2, 3, and 4; initial corrected engine speed, 11,200 rpm; cowl-lip-position parameter, 42°.

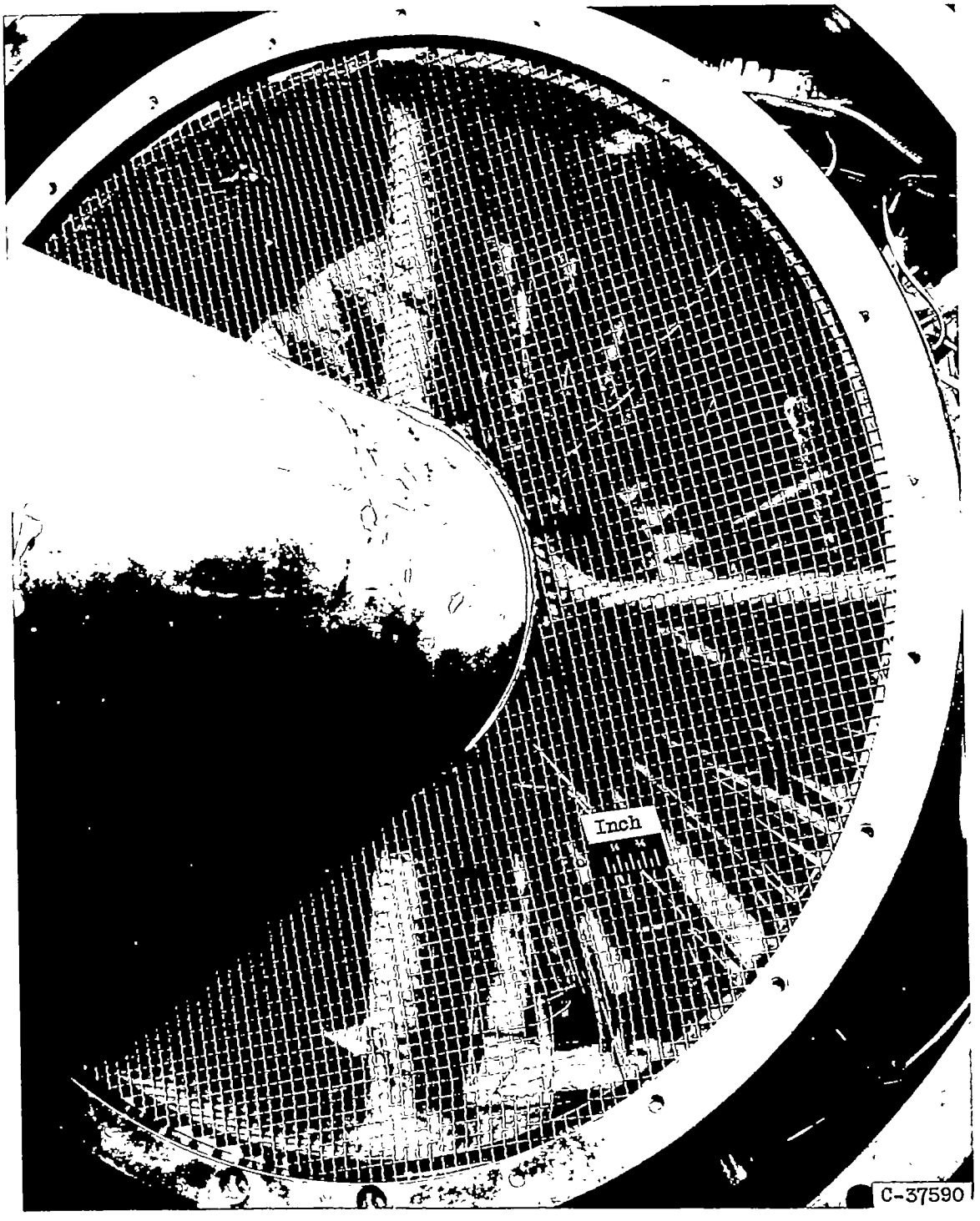

Figure 8. - Damage to compressor-inlet screen after firing of rockets 2, 3, and 4.